

Translational control of gene expression via interacting feedback loops

Liang Wang

Division of Mathematics, University of Dundee, DD1 4HN, UK

M. Carmen Romano

SUPA, Institute for Complex Systems and Mathematical Biology,

Department of Physics, Aberdeen AB24 3UE, UK and

Institute of Medical Sciences, University of Aberdeen, Foresterhill, Aberdeen AB24 3FX, UK

Fordyce A. Davidson

Division of Mathematics, University of Dundee, DD1 4HN

*Corresponding Author**

(Dated: March 24, 2022)

Translation is a key step in the synthesis of proteins. Accordingly, cells have evolved an intricate array of control mechanisms to regulate this process. By constructing a multi-component mathematical framework for translation we uncover how translation may be controlled via interacting feedback loops. Our results reveal that this interplay gives rise to a remarkable range of protein synthesis dynamics, including oscillations, step-change and bistability. This suggests that cells may have recourse to a much richer set of control mechanisms than was previously understood.

Keywords: translation, feedback, TASEP, oscillation, bistability

Control of gene expression refers to the processes by which the production of proteins is regulated by the cell. This is at the heart of the functioning of all living organisms and it allows cells to adapt to their environment. Control of gene expression can occur at multiple levels. In this Letter we focus on translational control.

Translation is the process by which a protein is made from a messenger RNA (mRNA) molecule. An mRNA consists of a sequence of codons, each coding for a certain amino acid. Translation is performed by molecular machines called ribosomes, which bind to the beginning of the mRNA (5' UTR region), scan it for the start codon and hop from one codon to the next, thereby producing the chain of amino acids which form the protein. When the ribosome reaches the stop codon, the protein is complete, is released into the cytoplasm and the ribosome binds off the mRNA.

Recent years have witnessed an explosion of information about how translational mechanisms regulate protein levels [1]. Prominent examples include translational control during cell stress [2] and switching in the mechanism responsible for translation initiation during the cell cycle [3].

Here we focus on one important case of translational control that has remained unexplored within this research framework, namely the interplay between positive and negative regulatory mechanisms. Translational negative feedback is caused by the ability of the produced proteins to bind to the 5'UTR region of their own mRNAs and hinder initiation [4, 5]. In fact, this

is the case for a crucial protein in the cell called PABP (PolyA Binding Protein), which promotes translation initiation and protects the transcripts from degradation enzymes [6–9]. On the other hand, virtually all mRNAs in the cell are subject to positive feedback via ribosome recycling due to their pseudo-circular structure [10], so that terminating ribosomes can be recycled back onto the same mRNA to commence a new round of translation. In this Letter, we show that the interplay between negative translational feedback and ribosome recycling gives rise to a novel range of dynamical behaviour in protein synthesis, including oscillations, step-change and bistability. Therefore, mRNAs for which the ubiquitous ribosome recycling positive feedback loop is augmented by negative translational feedback are endowed with a mechanism that allows them to finely tune protein synthesis according to environmental conditions.

Modelling framework.—Our mathematical framework is a multi-component model that accounts for translation, protein complex formation and binding of protein complexes and ribosomes at the 5'UTR (see Fig. 1).

Translation. We use a stochastic model of one-dimensional transport extensively studied in non-equilibrium statistical physics, called the Totally Asymmetric Simple Exclusion Process (TASEP) [11]. Ribosomes are represented by particles that hop stochastically along the sites of a one dimensional lattice, corresponding to the codons of the mRNA [12]. Traffic on the lattice can be classified into three main phases: the *low density* (LD) phase ($\alpha < \beta$, $\alpha < 1/2$), the *high density* (HD) phase ($\beta < \alpha$, $\beta < 1/2$) and the *maximal current* (MC) phase ($\alpha, \beta \geq 1/2$), limited by the initiation, exit and internal hopping rates, respectively. These phases have distinct average density, ρ , (average number of particles per site) and current, J , (average

* f.a.davidson@dundee.ac.uk

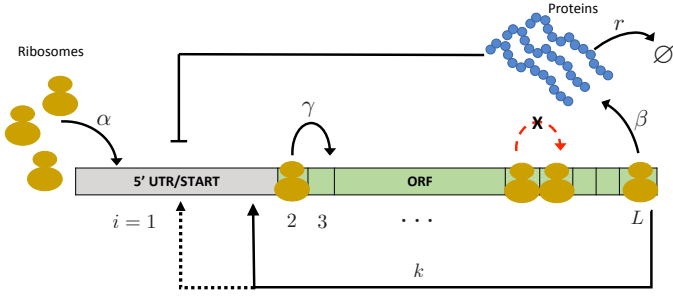


FIG. 1. Schematic of translation model with ribosome recycling and auto-negative feedback. Competitive recycling (dashed line), non-competitive recycling (solid line). Each site can be occupied by no more than one particle, so that at any time t the state at site i given by $S_i(t)$ is either $S_i(t) = 0$ or $S_i(t) = 1$, with $i = 1, \dots, L$, where L is the lattice length. Particles bind to the first site of the lattice at rate α , then hop from one site to the next at rate γ (usually rescaled to one and done so here) and finally leave the lattice from the last site at rate β , marking the point where the associated protein synthesis is completed. See text for further details.

number of particles hopping from one site to the next per unit time), which in the limit of an infinitely long lattice are given by: $\rho_{LD} = \alpha$, $\rho_{HD} = 1 - \beta$, $\rho_{MC} = 1/2$ and $J_p = \rho_p(1 - \rho_p)$, $p \in \{LD, HD, MC\}$ [13, 14].

Protein degradation. Once synthesised, proteins enter the intra-cellular pool, where they are subjected to degradation. Net removal from the protein pool is therefore reasonably modelled as a Poisson process with rate r . Hence, the average protein number in steady state is given by $N = N^* := J/r$.

Translational negative feedback. As detailed above, a protein can bind (often in multimeric form) to the 5'UTR of its own mRNA, thereby blocking the loading of ribosomes and thus repressing its own translation. Since protein binding/unbinding to the mRNA is generally much faster than ribosome loading [15], it follows after some analysis that the probability of the start codon being free for ribosome loading can be described by a Hill-function $f(N) = 1/(1 + (N/\theta)^n)$, where N is the protein copy number, θ measures the protein level that induces half maximal ribosome binding rate and n is the Hill coefficient measuring cooperativity of the protein multimer (see Supp. Mat.). Thus, the intrinsic initiation rate is modified from the standard constant rate, α , to $\alpha_F := \alpha f(N)$. Note that with the process in steady state, $N \equiv N^* = J/r$ and hence, we can write $f = 1/(1 + (4IJ)^n)$, where we have introduced the reciprocal factor $I := 1/(4\theta r)$ that measures *feedback intensity* (the factor of 4 is for algebraic convenience).

Translational positive feedback. The two ends of the mRNA can interact leading to a pseudo-circular struc-

ture [16], which together with the recycling complex Rli1p [17] promote terminating ribosomes to start a new round of translation on the same mRNA [18]. Following the approach in [19], a ribosome on site $i = L$ is assumed to either detach at rate β and enter the reservoir of free ribosomes or move directly onto site $i = 1$ at a *recycling rate* k (if $S_1(t) = 0$) to re-initiate the translation process.

Model for interacting feedback loops. Experimental results suggest that recycled ribosomes are channelled downstream of the normal *de novo* initiation site and thus may evade the blocking effect of the protein complex [20]. This is the case discussed here and referred to as *non-competitive recycling*. However, the relative position of the protein complex binding site and the recycled ribosome initiation site is not clear. Hence, in [21] we consider the alternative that both recycled ribosomes and *de novo* initiation are blocked by the protein complex, (*competitive recycling*) and compare the two mechanisms (see Fig. 1).

In the *non-competitive recycling* case we obtain the following mean-field equations (neglecting correlations between neighbouring sites) for the average occupancies ρ_i of the lattice sites

$$\frac{d\rho_1}{dt} = \underbrace{\alpha f(N)(1 - \rho_1)}_{\text{de novo}} + \underbrace{k\rho_L(1 - \rho_1)}_{\text{recycled}} - \rho_1(1 - \rho_2), \quad (1)$$

$$\begin{aligned} \frac{d\rho_i}{dt} &= \rho_{i-1}(1 - \rho_i) - \rho_i(1 - \rho_{i+1}), \quad i = 2, \dots, L-1, \\ \frac{d\rho_L}{dt} &= \rho_{L-1}(1 - \rho_L) - \beta\rho_L - \underbrace{k(1 - \rho_1)\rho_L}_{\text{recycled}}. \end{aligned}$$

By direct comparison with the standard TASEP, *effective* entry and exit rates can be defined as follows

$$\alpha_{eff} := \alpha f(N) + k\rho_L, \quad \beta_{eff} := \beta + k(1 - \rho_1). \quad (2)$$

Steady-state analysis of protein production and ribosome density.—Applying the mean-field TASEP approach to our model by imposing the conditions for each of the characteristic phases (LD, HD or MC) to the effective rates α_{eff} and β_{eff} leads to the derivation of analytical expressions for the protein production rate J and ribosome density ρ for each phase, as well as the phase boundaries (see Supp. Mat.). These analytical expressions agree well with Monte-Carlo simulations (see Fig. S1). This first analysis suggests that the long term dynamics of our model are unaltered from those of the standard translation model. However, a deeper analysis reveals that the complex interplay of the positive and negative feedback generates entirely novel dynamical responses.

Negative feedback and ribosome recycling induce oscillations in cellular protein level.—Monte-Carlo simulations reveal periodic oscillations in the number of

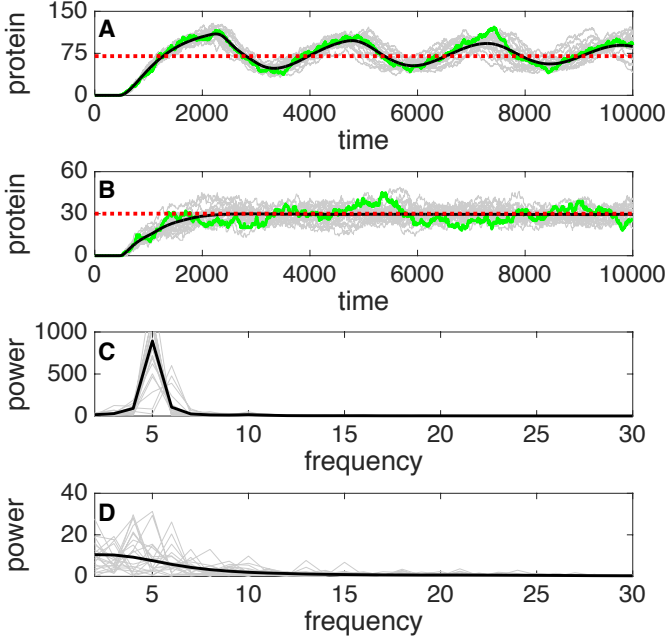


FIG. 2. Simulation and power spectrum of protein level in low density phase. (A,B) Protein number as a function of time. Averages over 5,000 realizations of stochastic simulations (black lines), 20 example realizations (grey lines), single example trajectory (green line). Red dashed lines are mean field N^* as computed using the steady state theory. Typical simulation (A) and the corresponding power spectrum (C) from the region where oscillations are predicted to exist ($\alpha = 0.8$). Typical simulation (B) and the corresponding power spectrum (D) from the region where oscillations are not predicted to occur ($\alpha = 0.05$). In all cases $\beta = 0.5$, $k = 0.2$, $I = 10$, $r = 0.002$, $n = 5$, $L = 500$.

proteins $N(t)$ within the initiation limited regime (LD phase). The stochastic nature of the individual simulations leads to slight fluctuations in the period of the oscillations making it difficult to systematically differentiate periodic oscillations from random fluctuations by visual inspection. However, a power spectrum analysis provides a clear demarcation: a tight, single-peaked spectrum is associated with the apparent periodic oscillations (Figs. 2A,C) whereas a broad band response is obtained in the case of stochastic fluctuations (Figs. 2B,D).

The appearance of oscillations is not wholly unexpected: the time needed for a ribosome to transit the mRNA naturally generates a delay between initiation and completion of protein synthesis. This generates a delay in the action of the negative feedback, a mechanism commonly known to generate oscillatory behaviour [22]. To get a better understanding, we formulated a simplified model for the protein copy number $N(t)$ in the LD

regime:

$$\begin{aligned} \frac{dN(t)}{dt} &= J(t) - rN(t) \\ &= \alpha_{eff}(t-T)(1 - \alpha_{eff}(t-T)) - rN(t), \end{aligned} \quad (3)$$

where T denotes the translational delay time [23]. Using Eq. 2 and $\rho_L = J/\beta_{eff}$, it follows that

$$\alpha_{eff}(t) = \frac{\alpha(\beta + k)}{\alpha k + \beta(1 + (4IrN(t))^n)}. \quad (4)$$

Substituting (4) into (3) results in a delay differential equation for N . The translational delay can be estimated as $T = L/(1 - \rho)$, where $\rho = \alpha_{eff}(N^*)$. This simplified model reproduces the amplitude and period of the stochastic simulations (cf. Fig. 2 A and Fig. S3D). Importantly, (3) is amenable to a stability analysis that allows us to identify conditions for the onset of oscillations. Indeed, it can be shown that on increasing α the steady state of (3) can be driven unstable via a Hopf bifurcation (see Supp. Mat.). After some algebra, it follows that the Hopf locus is an implicit expression of the form

$$B \cos(\sqrt{B^2 - r^2} T) + r = 0,$$

where B is a function of the system parameters. This locus forms a curve in the $\alpha - \beta$ -plane (see Fig. S2). After some algebra, it can be shown that necessary conditions for the existence of the Hopf locus are $n > 1$ and $I > F(\alpha, \beta, k, n)$, where F is a positive valued function of the parameters [21]. The condition $n > 1$ indicates that cooperativity in protein binding is necessary for the onset of oscillations, in accordance with [24]. The second condition indicates that the onset of oscillations occurs when the feedback intensity is sufficiently strong.

As we increase the feedback intensity, the Hopf locus shifts left in the $\alpha - \beta$ -plane, indicating that onset of oscillations occurs at lower values of the intrinsic loading rate α (see Fig. S2A), as one would intuitively expect. Interestingly, the Hopf locus also shifts left on increase the recycling rate (see Fig. S2B). Hence, counterintuitively, ribosome recycling - a positive feedback mechanism - *enhances* the onset of oscillations [25].

Interplay between recycling and negative feedback induces bistability in protein production. -In the MC and LD phases, the current J (and hence N^*) is uniquely defined for any given parameter set. On the contrary, in the HD phase $J = \beta_{eff}(1 - \beta_{eff})$ and after some algebra it can be shown that β_{eff} is the solution to the following $2n + 1$ degree equation (see Supp. Mat.):

$$4^n k I^n \beta_{eff}^n (1 - \beta_{eff})^{n+1} - (k\beta + \alpha)\beta_{eff} + \beta(\alpha + k) = 0. \quad (5)$$

In the absence of recycling ($k = 0$), Eq. (5) has the unique solution $\beta_{eff} = \beta$. In the absence of negative feedback ($I = 0$), β_{eff} is uniquely defined by $\beta_{eff} =$

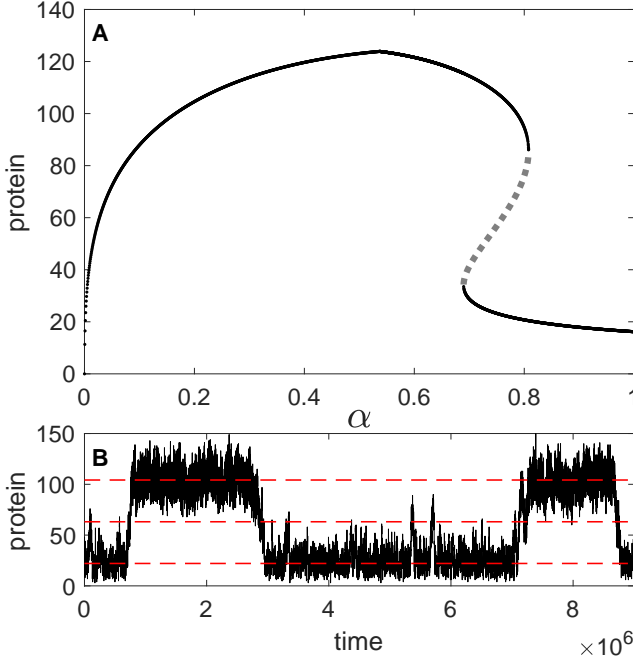


FIG. 3. (A) Protein number N^* as a function of the initiation rate α as predicted by the steady state theory. (B) Monte-Carlo simulation of protein number as a function of time (solid black line) with the mean field solutions N^* (red dashed lines) from A ($\alpha = 0.77$). In both cases $\beta = 0.015$, $k = 0.8$, $I = 24$, $r = 0.002$, $n = 2$, $L = 500$.

$\beta(\alpha + k)/(k\beta + \alpha)$ [19]. However, when both $k, I > 0$, Eq. (5) can have three admissible solutions, depending on the value of α (see Supp. Mat.). Thus, for suitably chosen parameters, there exists an interval of values of α for which three steady state values of $N^* = J/r$ co-exist. Figure 3A shows N^* as function of α , so that on increasing α from zero to one, the model transits from the LD to the HD phase. N^* is first monotonically increasing (LD phase). Then, at the LD/HD interface, N^* reaches a maximum, and within the HD phase N^* starts decreasing - the counterintuitive consequence of ribosome recycling as reported in [19]. As α is further increased, N^* passes through two fold bifurcations, leading first into, and then out of the interval of co-existent states - with the upper and lower branches separated by an intermediate, state indicated by the grey dashed line.

With values of α selected from the co-existence interval, simulations reveal that the time series of the number of proteins fluctuates about the high or low state on a time scale orders of magnitude larger than that of the fluctuations themselves. Rapid switching events between the favoured state are accompanied by a brief hiatus at the intermediate state. The mean locations of these favoured and intermediate states are well-approximated by the analytic expressions for the steady states obtained from Eq. 5 (Fig. 3B). Frequency histograms reveal the effect of varying α across the bistable region and together

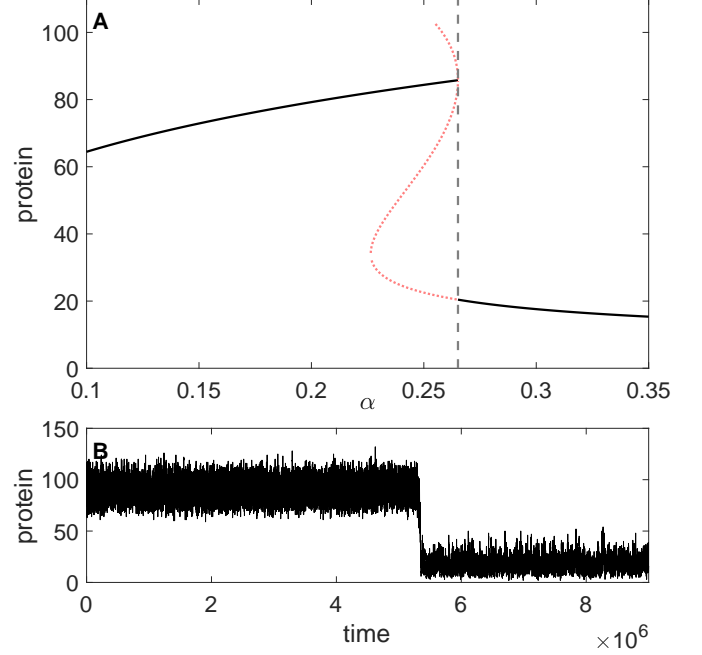


FIG. 4. Step-change in steady state protein levels. (A) Signal-response curve for protein number N^* as a function of the initiation rate α (black curves). Inadmissible solutions for (5) red dotted curve. The LD-HD boundary vertical grey dashed line. (B) Time series of the number of proteins: $\alpha = 0.28$ then switched to $\alpha = 0.3$ at time $t = 4.5 \times 10^6$. In each case $\beta = 0.015$, $k = 0.263$, $I = 24$, $r = 0.002$, $n = 2$, $L = 500$.

with dwell-time histograms indicate this to be a memory-less stochastic switching process (see Figs. S5 and S6)

Fixing k (resp. I) and increasing I (resp. k) increases the interval of values of α for which the fold exists (fold width - see Fig. S7). Interestingly, the location of the fold is also an increasing function of I and k . Indeed, somewhat counter-intuitively, for a fixed value of α , increasing the intensity of the negative feedback I , can force the system from a low N^* to a high N^* state. To understand this it is important to remember that the bistable region is located within the HD phase. Within the HD regime, any change of parameters leading to a decrease in the ribosome density leads to an increase in the ribosomal current (the lattice is less crowded and therefore particle flow is more efficient). As we increase the intensity of the negative feedback, the effective initiation rate α_{eff} decreases, thereby decreasing the density of ribosomes on the mRNA. Finally, we note that bimodality in protein production rate is a result of the balance between the negative and positive feedback loops and tuning one or the other can drive the system both into and out of a bimodal response (see Fig. S7).

Feedback interplay can induce step-changes in protein production—If we now fix the value of k so that

bistability is ensured, then a critical value of I exists at which the right boundary of the bistable region coincides precisely with the LD-HD boundary. In this case, as the initiation rate α passes through the LD-HD boundary, a discontinuity in the number of proteins occurs (Fig. 4A). [We obtain qualitatively the same behaviour by keeping I fixed and varying k .] This step-change in the number of proteins can be large, suggesting that small changes in the ribosome initiation rate α can result in a significant shift in protein levels. Simulations confirm this theoretical prediction. On increasing α dynamically during a simulation, a step change (around 75% reduction) is clearly apparent on transept of the LD/HD critical value (Fig. 4B). This cliff-edge response is another unique feature of resulting from the interplay between feedback and recycling.

Conclusions.—Our model suggests that negative and

positive feedback acting together in translation may provide cells with a versatile mechanism to adapt their protein levels according to the environment. Moreover, as mentioned above, the centrally important protein PABP is subject to ribosome recycling and is known to exhibit translational negative feedback. Hence, understanding how its production is controlled is important to gain insight into translational control at the global level. Interestingly, PABP has also been implicated in circadian oscillations [26]. The oscillatory behaviour predicted by our model could therefore play an important role in this fundamental regulatory mechanism. Finally, disturbances of poly(A) tail length have been linked to a number of physiological and pathological processes. Therefore, a better understanding of the interplay of ribosome recycling and translational negative feedback has far reaching consequences.

-
- [1] J. Hershey, N. Sonenberg, and M. Mathews, *Cold Spring Harb Perspect Biol.* **4**, a011528 (2012).
 - [2] K. Spriggs, M. Bushell, and A. Willis, *Mol. Cell* **40**, 228 (2014).
 - [3] S. Pyronnet, J. Dostie, and N. Sonenberg, *Genes Dev.* **15**, 2083 (2001).
 - [4] C. Brunel, P. Romby, C. Sacerdot, and et al., *J. Mol. Biology* **253**, 277 (1995).
 - [5] R. Betney, J. de Silva, and I. Stansfield, *RNA-A* **16**, 655 (2010).
 - [6] D. Cao and R. Parker, *RNA* **7**, 1192 (2001).
 - [7] E. Hornstein, H. Harel, G. Levy, and O. Meyuhas, *FEBS Letters* **457**, 209 (1999).
 - [8] O. Neto, N. Standart, and C. Desa, *Nucleic Acids Research* **23**, 2198 (1995).
 - [9] J. Bag, *J. Biol. Chem.* **276**, 47352 (2001).
 - [10] S. Wells, P. Hillner, R. Vale, and A. Sachs, *Mol. Cell* **2**, 135 (1998).
 - [11] B. Derrida, E. Domany, and D. Mukamel, *J. Stat. Phys.* **69**, 667 (1992).
 - [12] C. MacDonald, J. Gibbs, and A. Pipkin, *Biopolymers* **6**, 1 (1968).
 - [13] B. Derrida, M. Evans, C. Hakim, and V. Pasquier, *J. Phys. A: Math. Gen.* **26**, 1493 (1993).
 - [14] G. Schütz and E. Domany, *J. Stat. Phys.* **72**, 277 (1993).
 - [15] L. Chen, R. Wang, T. Kobayashi, and K. Aihara, *Phys. Rev. E* **70**, 011909 (2004).
 - [16] D. Barthelme, S. Dinkelaker, S.-V. Albers, P. Londei, U. Ermler, and R. Tampe, *Proc. Natl Acad. Sci.* **108**, 3228 (2011).
 - [17] C. Shoemaker and R. Green, *Proc Natl Acad. Sci.* **108**, 1392 (2011).
 - [18] N. Amrani, S. Ghosh, D. Mangus, and A. Jacobson, *Nature* **435**, 1276 (2008).
 - [19] E. Marshall, I. Stansfield, and M. Romano, *J. R. Soc. Interface* **11**, 104 (2014).
 - [20] L. Rajkowitsch, C. Vilela, K. Berthelot, C. Ramirez, and J. McCarthy, *J. Mol. Biol.* **335**, 71 (2004).
 - [21] L. Wang, M. Romano, and F. Davidson, In preparation.
 - [22] S. Pigolotti, S. Krishna, and M. Jensen, *Proc Natl Acad. Sci.* **104**, 6533 (2007).
 - [23] Note that in agreement with numerical simulations, we only expect oscillations within the LD phase, since in both HD and MC, the current J is independent of the delay between loading and exit (see Supp. Mat.).
 - [24] M. Elowitz and S. Leibler, *Nature* **403**, 335 (2000).
 - [25] B. Ananthasubramaniam and H. Herzog, *PLoS ONE* **2014**, e104761 (2014).
 - [26] S. Kojima, E. Sher-Chen, and C. Green, *Gene Dev.* **26**, 2724 (2012).